ACCELERATION OF GRAPHITISATION IN CARBON STEELS TO IMPROVE MACHINABILITY

D.V. Edmonds and K. He - Institute for Materials Research, University of Leeds, LS2 9JT, UK

ABSTRACT

It is generally believed that exchanging the metastable cementite phase in carbon steel for graphite should improve machinability, and also result in better cold workability. However, the annealing times required are generally too long to suit the industrial processing of a high volume product and so other routes are used, for example, the addition of elements such as Pb, S, Se, Te, Bi and P, some of which impair cold forgeability. In the present work the graphitisation process has been accelerated by alloying with Si and Al. Metallographic analysis of the graphitisation process, including high resolution microanalytical EELS, has revealed information on the formation of the graphite nodules and also on the accompanying dissolution of the cementite phase. Emphasis is placed upon the stability and dissolution of cementite during annealing, on which it is suspected that the graphite phase can nucleate, and evidence is provided to support this hypothesis. Different formation behaviour and kinetics of the graphite nodules has also been detected between different starting microstructures, for example, between bainite and martensite. Consequently, different graphite nodule dispersions may result from a different starting microstructure, as well as a different time to complete the graphitisation process. The results of tensile tests show adequate softness and ductility of the graphitised steel, which is thus expected to give good cold forging properties.

KEYWORDS

Carbon steel; Graphitisation; Si and Al alloying; Graphite; Cementite; Martensite; Bainite; EELS; EFTEM; Mechanical properties.

INTRODUCTION

World annual steel production is currently in excess of one billion metric tons, and because of its reliability and cost-effectiveness in a wide range of engineering applications, a significant fraction of this will be carbon steels, of which a sizeable proportion will undergo cold working and/or machining at some stage of the manufacturing cycle. In order to improve machinability (to produce free-cutting grades) the addition of Pb, usually in combination with S, is customarily made. Alternative alloying is also practiced: traditional additives include Se, Te, Bi and P, some of which (along with Pb) require special controls during steelmaking in order to reduce exposure to toxic fume, and some of which impair cold forgeability.

The microstructure of carbon steels is ferrite/carbide (cementite), the exact fraction and distribution of the phases depending upon the heat treatment: normalised to a ferrite/pearlite condition, or cooled/austempered to bainite, or quenched to martensite and tempered. The presence of cementite will generally limit the cold working properties. By transforming the ferrite/cementite structure to a ferrite/graphite structure, both the machinability and cold forgeability can be improved, and at the same time, after first softening by graphitisation, the strength can be regained by dissolving graphite into austenite and quenching, a procedure suitable for some parts that require high strength but are difficult to machine [1,2]. This practice has been used successfully since the 1940's for cast irons, but has not been developed for steels because of the long annealing times required, generally of the

HOME

order of tens or hundreds of hours [3,4], unrealistic to include in a high-volume production schedule. However, legislation such as the European Directive on End-of-Life Vehicles, intended to reduce the amount of Pb, amongst other hazardous materials, in vehicles, has focused efforts on trying to reduce the annealing times required by accelerating the kinetics of graphitisation.

If it is assumed that the graphitisation process during the annealing of a carbon steel consists of two steps, the dissolution of cementite and the nucleation of graphite, then it appears that the various approaches adopted to accelerate graphitisation, based upon alloying, can be considered to fall into two categories, either destabilisation of the cementite phase, or the provision of heterogeneous nucleation sites for the graphite. The former approach has generally centred upon alloying with Si, which element reduces the stability of cementite, whilst also avoiding or reducing alloying elements such as Mn and Cr, which increase cementite stability [5-8]. The latter approach considers additions which will provide a variety of nucleating particles, for example, non-metallic inclusions, such as Al_2O_3, SiO_2 or silicates, and nitrides and carbides such as BN, AlN, TiN, ZrN, Nb(C,N) and V(C,N), or sulphides, have all been promoted as nucleating sites for graphite [5,6,9,10]. The philosophy of providing nucleating particles to promote graphite formation can be successful, but can be difficult to control, for example, BN appeared to be very effective in nucleating graphite [5,6], although the BN particles segregate in the austenite grain boundaries, so that graphite phases nucleated on these BN particles can be non-uniformly distributed.

The work described here and the evolving graphitisation methodology suggested, essentially combines both approaches: firstly, Si (combined with Al) alloying in steels with reduced Mn content, is used to destabilise cementite, whilst it is proposed that the graphite can nucleate upon the prior, but dissolving, cementite particles, avoiding the need to make special additives for this purpose. A corollary of this methodology is that the mode of formation of the cementite particles thus assumes some importance, that is, whether they form as a constituent of pearlite, bainite or tempered martensite [11].

In the present study, the graphitisation process is examined by both light optical and electron microscopy, including high-resolution analytical techniques: electron energy loss spectroscopy (EELS) and energy-filtered transmission electron microscopy (EFTEM). The starting microstructure is taken into account and the nucleation of graphite nodules on inclusion particles is also observed. Finally, the mechanical properties of the graphitised experimental steel were recorded.

MATERIALS AND EXPERIMENTAL METHODS

Compositions of the experimental steels are given in Table 1. A 50g argon-arc melt was made from high-purity elements under a partial pressure of argon gas, and then homogenised at 1150°C in an argon gas atmosphere for 70 hours and water quenched. A 50kg vacuum melt was made at Swinden Technology Centre, Corus Group, Rotherham, UK, and half the cast was reheated and forged to 32mm diameter bar, from which Jominy end-quench specimens were machined. The Jominy

Table 1 Compositions of experimental steels (wt.%)

Steel	C	Si	Mn	P	S	Al	N	B
A: 50g Si-Al	0.38	1.82	0.07	nd	nd	1.44	nd	nd
B: 50kg Si-Al	0.39	1.76	0.012	0.008	<0.005	1.28	0.009	0.0006
nd = not determined								

were reheated to 1150°C for 0.5 hours in an argon atmosphere before end quenching (Fig. 1) to produce a range of starting microstructures along the length of the bar, in the same steel, which could then be subjected to graphitisation annealing. Graphitisation annealing was carried out at 680°C for various times. Standard techniques were used to prepare specimens for examination by light and scanning electron microscopy (SEM). Scanning electron microscopy examination was carried out on a Camscan Series 4 instrument with an Oxford ultra-thin window EDX attachment and ISIS software, operating at 20kV. Samples for transmission electron microscopy (TEM) were first mechanically ground to a thickness of ~80μm from thin slices, followed by electropolishing in a twin-jet unit using an electrolyte of 10% perchloric acid, 30% 2-butoxyethanol and 60% ethyl alcohol, at 20mA, 15V and ~-10°C. TEM examination and microanalysis were carried out in a Philips CM 20 with EDX attachment, operating at 200kV, or a CM200 FEGTEM with EDX and EELS attachment, beam energy 197kV. EELS spectra were recorded using a Gatan Imaging Filter 200. Processing was performed using Gatan Digital Micrograph and EL/P software.

Specimens for mechanical testing were prepared as follows: 10mm×15mm×72mm sections of steel bar were treated at 1200ºC for 1 hour in argon gas and water quenched, and then annealed at 680ºC for various times. Tensile samples were machined according to the Hounsfield Tensometer (type W) instruction and tensile tests carried out using a Hounsfield Tensometer machine (type W).

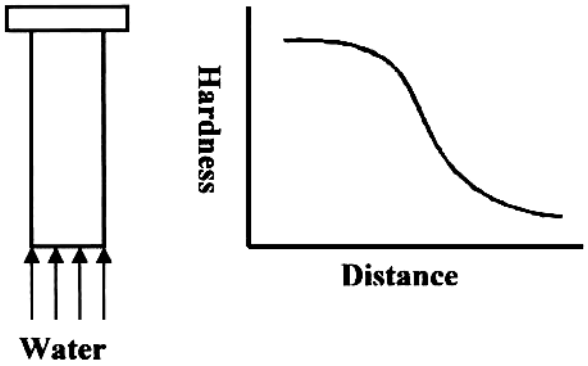

Fig. 1 Schematic diagram illustrating the Jominy end-quench treatment and a typical hardness versus distance profile along the length of the Jominy bar, from the quenched end, reflecting variation in the microstructure.

RESULTS AND DISCUSSION

The evolution of the microstructure in the quenched argon-arc melt samples during graphitisition annealing was followed by both light optical microscopy and transmission electron microscopy, from the formation and dissolution of cementite to the nucleation and growth of graphitic nodules. In these samples, the as-quenched starting matrix microstructure is martensite with scattered aluminium nitrides and oxides (Fig. 2(a)), but this rapidly tempers during heating and short times at the annealing temperature of 680ºC. After 0.5 hours at the annealing temperature, coarse cementite particles are still present, mainly situated at the interfaces of prior martensite plates, which are still visible (Fig. 2(b)). Graphite particles have already formed (Fig. 2(c)), but at this stage these particles were associated with the aluminium nitride or oxide inclusions (Fig. 2(d)), and were thus unevenly dispersed and fairly coarse. After annealing times closer to 1 hour in this experimental steel, most of the original cementite particles had dissolved. After 1.5 hours virtually all of the identifiable cementite particles had decomposed and been replaced by graphite nodules. After ~2

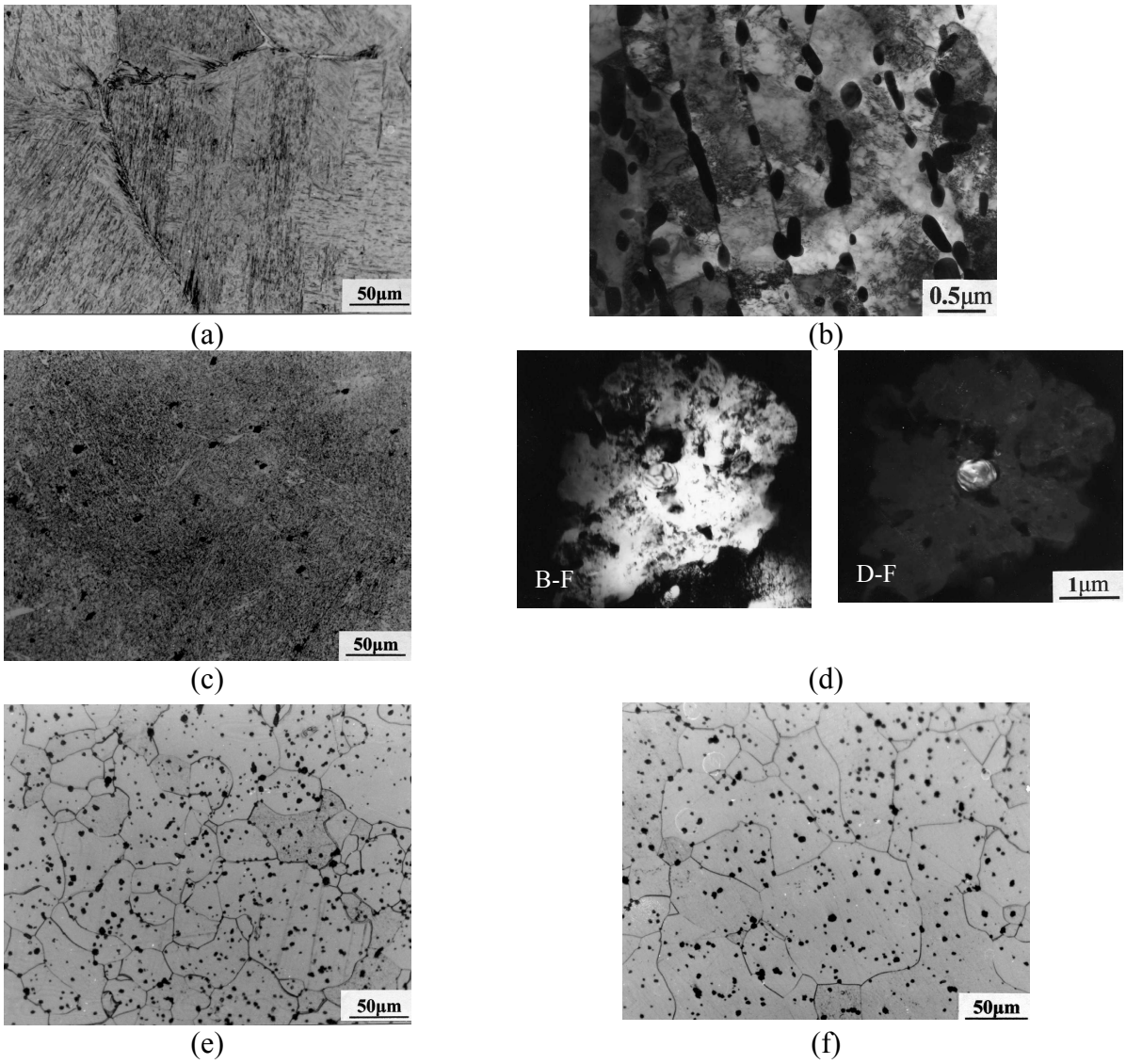

Fig. 2 Micrographs showing the graphitisation process in steel A: (a) light optical micrograph of starting as-quenched martensitic microstructure; (b) dense distribution of cementite particles in tempered martensite after 0.5 hours (TEM); (c) light optical micrograph showing a coarse distribution of graphite nodules after 0.5 hours; (d) a large irregular graphite nodule containing a coring particle (TEM bright-field (BF) image and corresponding dark-field (DF) image using the (-1 0 1) AlN reflection); (e) light optical micrograph showing a denser distribution of graphite nodules formed after 3.5 hours; (f) light optical micrograph showing the distribution of graphite nodules after 55 hours.

hours or longer (Figs. 2(e) and (f)), the distribution and size of the graphite nodules did not show much change, suggesting that graphitisation was virtually complete after this time and that the graphite nodules were relatively resistant to coarsening under these conditions. These results demonstrate that the alloying philosophy adopted enabled acceleration of the graphitisation process in the experimental steel such that it was virtually complete within ~2-3 hours, significantly faster than has generally been recognized previously .

An important additional observation made by TEM was that two distinctly different types of graphite nodule appeared to be present; coarse ones with an irregular morphology formed early in the annealing process, and nucleated on existing inclusion particles in the steel, as described above,

but also smaller, and more regularly-shaped spheroidal ones, apparently lacking a coring particle, as illustrated in Fig. 3 [12]. These latter nodules formed the bulk of a more refined dispersion, with diameters in the range of 2-5μm after graphitisation was complete.

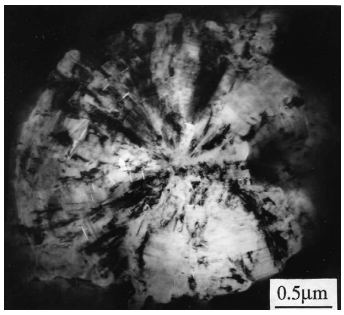

Fig.3 TEM micrograph of a smaller spherical graphite nodule, after 3.5 hours in steel A.

The question thus arises as to how the smaller graphite nodules nucleate, and some evidence for a possible mechanism was suggested by the unexpected observation that many of the cementite particles still surviving after about 1 hour, were not wholly crystalline cementite, but were more complex (Fig. 4): EDX analysis and electron diffraction analysis revealed that one part was non-crystalline and carbon-rich whilst one part was crystalline Mn-rich cementite. The average Mn content of the crystalline part was 2 at%, much higher than that of the cementite particles observed after annealing for only 0.5 hours, which was closer to the bulk Mn concentration in the experimental steel.

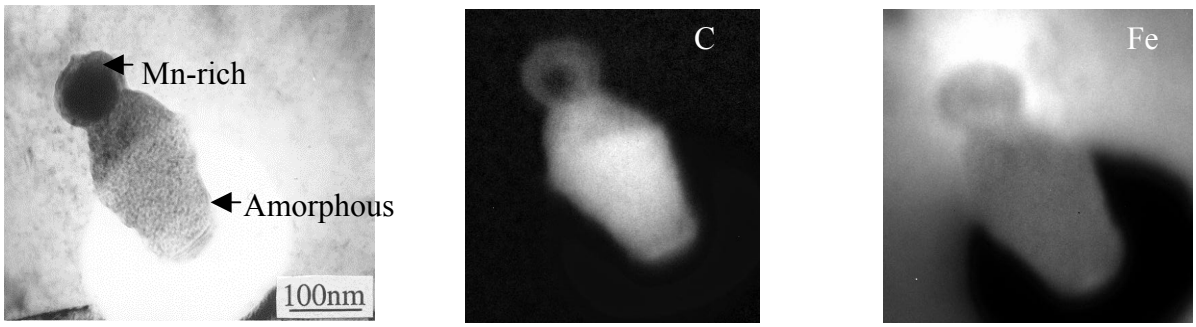

(a) (b) (c)

Fig 4. (a) TEM BF image showing a complex particle with a C-rich amorphous part and a smaller Mn-rich crystalline cementite part, and (b) C K- and (c) Fe $L_{2,3}$-edge EFTEM jump-ratio images from steel A after 58 minutes.

Electron energy loss spectroscopy (EELS) has been used to analyse these complex particles, as well as other phases involved in the graphitisation process. Figure 5 presents the carbon K-edges collected from cementite, crystalline and non-crystalline parts of complex particles and a graphite nodule. The carbon K-edge of the carbon-rich part of the complex particle suggests that this region is amorphous, which could be considered as an intermediate stage during the overall graphitisation process. This implies that the cementite itself could be involved in the nucleation of graphite nodules, in particular, the spherical graphite nodules mentioned above, which apparently form without a coring particle [12].

Supportive evidence for this hypothesis has been obtained by mapping the EELS plasmon energy loss shifts across the small regular spheroidal graphite nodules [13], which indicates a near-

amorphous core surrounded by an outer mantle that is largely graphitic in character. This would be likely to follow if the amorphous regions described above formed the nucleus for the nodules.

Additional support for the importance of the dissolving cementite to formation of the nodules is also gained from the different graphitisation behaviour observed between different starting microstructures [11], for example, between martensite and bainite, typically appearing as in Fig. 6. It is likely that the nature of the carbides forming in these two microstructures should be different, and play a more decisive role in determining graphitisation, than the ferritic matrix, which after annealing at 680ºC might be expected to be fairly similar despite different origins from the austenitic state. This difference in graphitisation behaviour was identified by annealing the end-quenched Jominy bars, which has the immediate experimental advantage of comparing the behaviour in the same heat-treated steel specimen. Figure 7 highlights the quantitative difference in graphitisation on progression away from the martensitic quenched-end, through the bainitic region. The graphite nodule dispersion formed within the bainite microstructure is more refined.

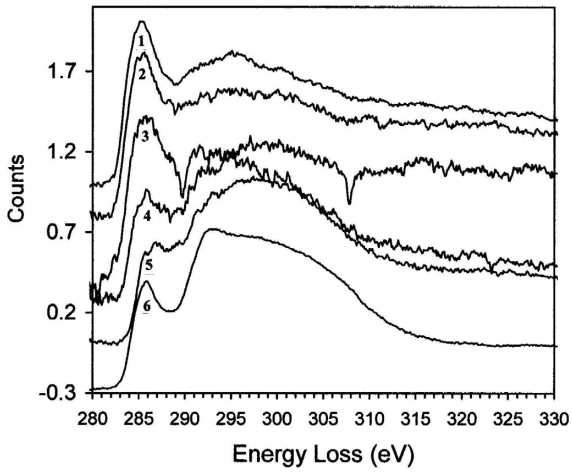

Fig. 5 EELS spectra of carbon K-edge ranging from cementite to graphite: (1) cementite reference; (2) cementite part of complex particle 1; (3) cementite part of complex particle 2; (4) amorphous part of complex particle 1; (5) amorphous part of complex particle 2; (6) graphite, formed by annealing steel A at 680ºC.

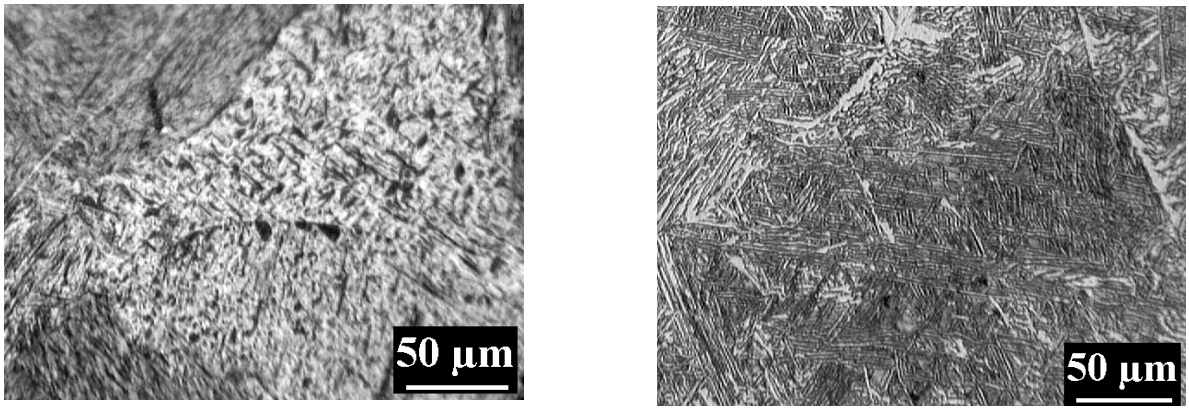

(a) (b)

Fig. 6 Light optical micrographs of different starting microstructures along a Jominy end-quench bar from steel B: (a) martensitic structure; (b) bainitic structure.

TEM showed that, in the martensite region, transitional carbides, identified by electron diffraction as epsilon carbide, precipitated first during the early stage of tempering (Fig. 8), and were then displaced by cementite that subsequently coarsened prior to dissolution. In contrast, observations of the bainitic region suggested that cementite was the first carbide to precipitate, rather than epsilon carbide. It was also observed that the time for completion of graphitisation in martensite lagged behind that in the bainite region by at least half an hour, although the cementite particles formed during annealing had similar sizes in both martensite and bainite regions. Of importance also, is the fact that no graphite nodules were observed to contain a coring particle in the bainite region

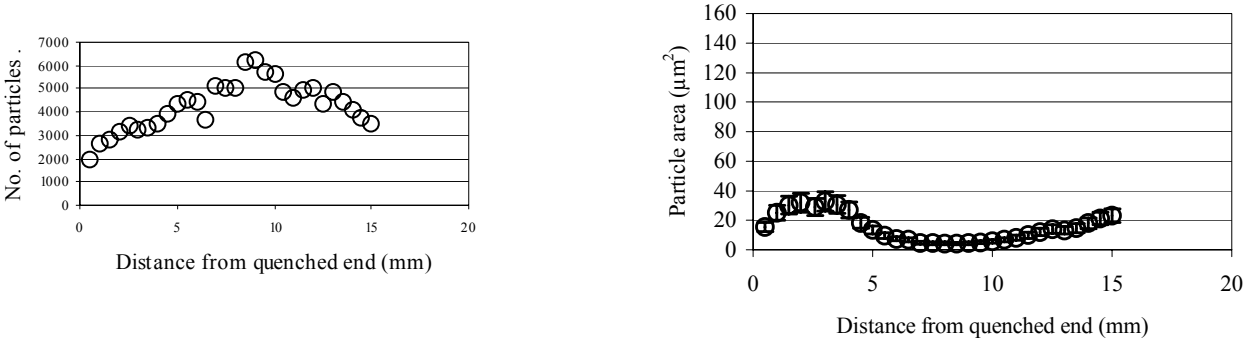

(a) (b)

Fig. 7 (a) Number, and (b) area of individual graphite particles, along a Jominy bar from steel B after annealing for 6 hours at 680ºC. (Martensite extends approximately 4 mm from the quenched-end and bainite to approximately 15 mm from the quenched-end.) After [11].

whereas aluminium nitrides and oxides actively nucleated graphite in the martensite region, where graphite nodules both with and without coring particles were observed. Furthemore, in the bainite region, a denser distribution of graphite nodules, with a finer size, was produced as compared with that in the martensite region. These features are illustrated in Fig. 9. These results further demonstrate that there must be another nucleation mechanism operating, which is thought to be associated with the cementite particles, and dependent upon their chemistry and stability, as determined by alloying and formation route.

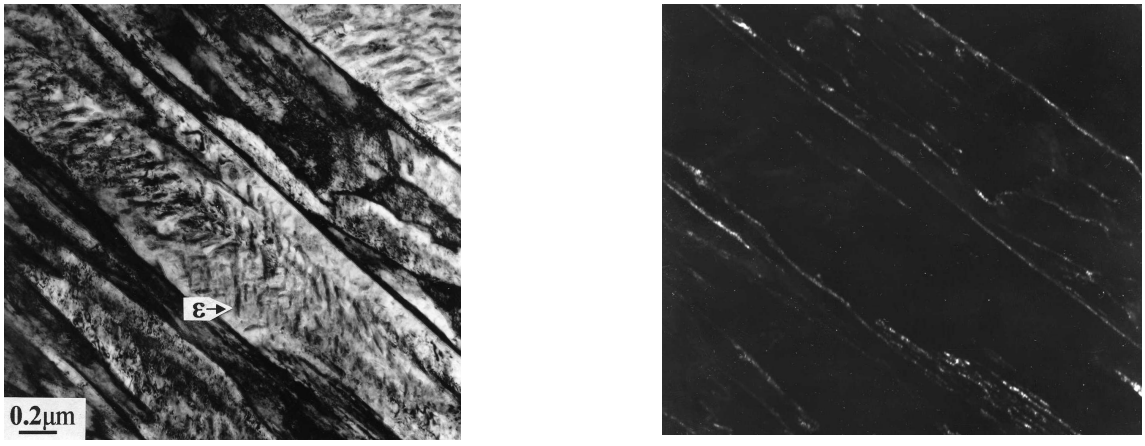

(a) (b)

Fig. 8 TEM images of starting microstructure showing the presence of epsilon carbides within martensite laths and interlath retained austenite films in the martensite region of an end-quenched Jominy bar from steel B: (a) BF image; (b) DF image using $(200)_\gamma$ reflection showing retained austenite films.

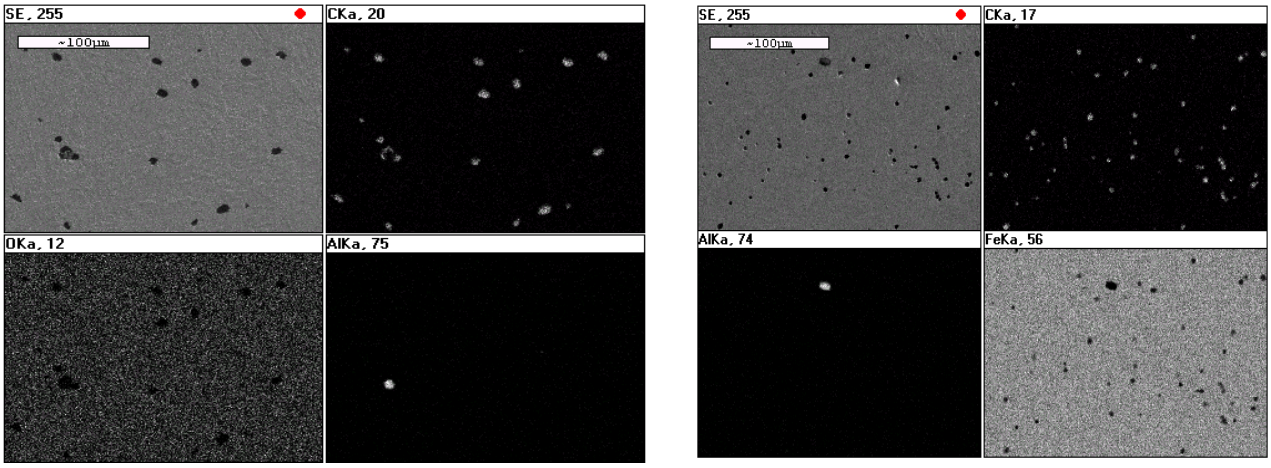

(a) (b)

Fig. 9 SEM X-ray mapping showing graphite nucleation at a pre-existing particle, and the distribution of graphite nodules between martensite and bainite regions in an end-quenched Jominy bar from steel B: (a) AlN acting as the nucleus for a graphite nodule in a martensite region; (b) a denser distribution of finer graphite nodules in the bainite as compared with the martensite region, and evidence that an AlN particle has not acted as a nucleant for graphite nodules.

The mechanical properties of experimental steel B, annealed for various times, are given in Table 2. This shows that graphitisation annealing of the experimental steel produced a soft steel with good ductility. The properties are also broadly comparable with those recorded in the literature for similar steels which show good machinability combined with good cold forgeability.

Table 2. Mechanical properties of experimental steel B after various graphitisation annealing times, and results for customary and experimental free-cutting steels for comparison.

Steel	Time (h)	Yield Stress (MPa)	UTS (MPa)	RA (%)	EL (%)	Ref.
Experimental steel B	3	278	365	57.2	33.1	-
Experimental steel B	24	216	347	58.4	30.5	-
Experimental steel B	96	156	258	55.5	30.2	-
0.35C graphitised steel	-	223	343	-	42	1
SAE 12L14	-	289	409	57	36	14
Experimental Pb-free steel	-	298	401	57	36	14

SUMMARY

By alloying with Si and Al, graphitisation at 680ºC in a medium-carbon steel has been accelerated such that the process is virtually complete within ~2-3 hours. The fastest graphitisation is effected from a bainitic starting microstructure, and is believed to be due to the different route by which cementite forms in this structure compared with starting from a quenched martensite: a more refined distribution of graphite nodules with a finer size is also produced. The importance of cementite suggested by this work is because some evidence was found that can be interpreted to support the hypothesis that graphite nodules may nucleate upon the carbide as it is dissolving at the annealing temperature, the stability of the cementite phase having been reduced by the alloying elements.

Metallographic examination of the microstructural evolution during graphitisation, including EELS analysis of the carbon K-edges of the phases involved in graphitisation, demonstrated that cementite can be involved in the nucleation and formation of graphite nodules. Nodules so-nucleated were small and regular, when compared with those nucleated on other particles, for example, AlN present in these experimental steels, which were coarse and irregularly-shaped. An important conclusion, therefore, is that alloying to de-stabilise the cementite phase, which provides the carbon, is more important to reducing the graphitisation time in carbon steels than providing heterogeneous nucleation sites for the graphite nodules. Mechanical property measurements from the graphitised steel showed adequate softness and good ductility, which would be expected to result in good cold forging properties.

ACKNOWLEDGEMENTS

This work was partly funded under EPSRC grants, reference GR/M33693 and GR/R95708. We are grateful to our colleagues R. Brydson and A. Brown for assistance with EELS analysis, to M.J.W. Green and P.E. Reynolds at Swinden Technology Centre, Corus Group plc, Rotherham, UK, for supplying experimental steels and carrying out the Jominy heat treatments and measuring graphite distributions, and to S. Hersey for performing the mechanical tests.

REFERENCES

1) K. FUKUI and N. MIZUI, High-Strength Sheet Steels for the Automotive Industry, Iron and Steel Society/AIME, USA, Baltimore (1994), p.171.
2) S. KATAYAMA and M. TODA, Machinability of medium carbon graphitic steel, J. of Mater. Processing Technol. 62, (1996), p.358.
3) C.R. AUSTIN and M.C. FETZER, Factors Controlling Graphitization of Carbon Steels at Subcritical Temperatures, Trans. of the A.S.M. 35, (1945), p.485.
4) R.H. HICKLEY and A.G. QUARRELL, J. Iron Steel Inst. 178, (1954), p.337.
5) T. IWAMOTO, T. HOSHINO. K. AMANO and Y. NAKANO, Fundamentals and Applications of Microalloying Forging Steels, Minerals, Metals and Materials Society/AIME, Golden (1996), p.227.
6) T. MEGA, R. MORIMOTO, M. MORITA and J-I. SHIMOMURA, Surface and Interface Analysis (UK), 24, (1996), p.375.
7) W.C. LESLIE and G.C. RAUCH, Metall. Trans. 9A, (1978), p.343.
8) H.J. GOLDSCHMIDT, Interstitial Alloys. Butterworths, London (1967), p.117.
9) T. HOSHINO, T. IWAMOTO, A. MATSUZAKI and K. AMANO, Kawasaki Steel Corporation, Japan, US Patent 5,648,044 (1997).
10) New Technology Japan. 26, (1999), p.29.
11) K. HE, D.V. EDMONDS, M.J.W. GREEN and P.E. REYNOLDS, Materials Science and Technology, MS and T 2004; Volume 1: AIST Process Metallurgy, Product Quality and Applications Proceedings, New Orleans, LA (2004), p.207.
12) K.HE and D.V. EDMONDS, 15th International Congress on Electron Microscopy, Proceedings vol. I. Physical, Materials and Earth Sciences, ed. R. Cross and M. Witcomb, Microscopy Society of Southern Africa, Durban (2002), p.719.
13) K.HE, A. BROWN, R. BRYDSON, H.R. DANIELS and D.V. EDMONDS, 13th European Microscopy Congress, Antwerp, Belgium, August 2004. vol II: Materials Sciences ed: G. Van Tendeloo, Belgian Society for Microscopy, Liege (2004), p.591-592.
14) I. TAKASHI and M. TOSHIYUKI, JFE Technical Report (2004), p.74.

HOME